Article

Journal of
Nanoscience and Nanotechnology
Vol. 16, 3961–3964, 2016
www.aspbs.com/jnn

Enhanced Red Upconversion Luminescence in Yb–Er Codoped $NaYF_4$ Nanocrystals

Weiye Song, Xueqing Bi, Xingyuan Guo, Shushen Liu, and Weiping Qin*

State Key Laboratory on Integrated Optoelectronic, College of Physics, College of Electronic Science and Engineering, Jilin University, Changchun 130012, China

In this work the effects of $NaYF_4$:Yb,Er (NYE) structure on the enhanced red upconversion luminescence (UC) was investigated. α-NYE nanocrystals (NCs) and β-NYE NCs were fabricated by a high temperature decomposition reaction method. The prepared NCs were characterized by X-ray diffraction (XRD), transmission electron microscopy (TEM), and photoluminescence (PL) spectroscopy. The results show that the red UC luminescence of α-NYE NCs is significantly enhanced compared with that of β-NYE. Furthermore, a possible energy transfer mechanism was proposed on the basis of our experimental results.

Keywords: Upconversion Luminescence, $NaYF_4$, Nanocrystals, Rare Earth Ions.

1. INTRODUCTION

In recent years extensive researches have been carried out to investigate the optical properties of rare earth (RE) doped luminescent materials and to discover their potential applications due to their UV-Vis-IR luminescence. Much attention has been especially paid to the study of RE doped upconversion (UC) phosphors, which emit visible light via absorption of lower energy photons.[1–3] Nowadays, luminescent materials that are activated by lanthanide ions have many potential applications in biological detection,[4–6] low-intensity IR imaging,[7–10] photocatalysis.[11–13]

$NaYF_4$ has been regarded as the most efficient upconversion host material due to low quenching of the excited states of RE ions due to lower phonon energy.[14,15] Compared to quantum dots and traditional organic dyes pumped by ultraviolet radiation, RE doped UC phosphors possess narrow emission lines, low photobleaching, no-autofluorescence, deep penetration, and low light scattering.[16] A number of synthesis methods are available, including solid treatment,[17] co-precipitation in aqueous phase,[18] soft and hard template routes,[19] and a solvothermal method.[8] However, the fabrication of monodisperse nanocrystals (NCs) with diameter of ∼10 nm remains a challenge. In order to control the shape, size, and phase structure of NCs, organic additives functioning as "shape modifiers" are favored because they either promote or inhibit crystal growth through dynamically modifying the crystal facets.[20] Therefore, they are part of cost-effective and environmentally-friendly synthetic methods that become more popular for obtaining monodisperse nanocrystals.

In this work, the Er–Yb codoped α-and β-$NaYF_4$ UC NCs with an average of ∼10 nm were synthesized using a facile hydrothermal method. With the introduction of different phase structure, enhanced red UC emission was observed as a result of non-resonant energy transfer between Er^{3+} and Tm^{3+} and the possible energy transfer mechanism was proposed.

2. EXPERIMENTAL DETAILS

2.1. Materials

$RECl_3 \cdot H_2O$:Yttrium chloride ($YCl_3 \cdot 6H_2O$), Erbium chloride ($ErCl_3 \cdot 6H_2O$), Ytterbium chloride ($YbCl_3 \cdot 6H_2O$) were obtained from Shandong Yutai Fine Chemical Factory with 99.999% purity. 1-Octadecene (ODE, 90%) and oleic acid (OA, 90%) were purchased from Alfa Aesar. NaOH (98%), NH_4F (98%) were supplied by Shanghai Chemical Reagent Company. All other chemicals were of A. R. grade and used as received without further purification.

2.2. The Synthesis of α-$NaYF_4$:Yb,Er Nanocrystals (α-NYE NCs)

α-NYE NCs were synthesized via the thermal decomposition method previously described.[20] Briefly, 0.242 g of

*Author to whom correspondence should be addressed.

1533-4880/2016/16/3961/004 doi:10.1166/jnn.2016.11866

$YCl_3 \cdot 6H_2O$, 0.0697 g of $YbCl_3 \cdot 6H_2O$, 0.0076 g of $ErCl_3 \cdot 6H_2O$ were added to a mixture of 7.5 mL of OA and 15 mL of ODE in a four-necked flask at room temperature and then heated to 150 °C under nitrogen. After half hour the mixture was cooled to room temperature. 0.16 g of NH_4F and 0.1 g of NaOH were previously dissolved in methanol, and then transferred dropwise into the above solution over a period of 40 min at a proper flow rate, while the temperature was maintained at 50 °C. Then, the reaction mixture was heated to 290 °C and kept at this temperature for 60 min under nitrogen protection. After that, the mixture was cooled down slowly to room temperature. The product was centrifuged and washed with deionized water and ethanol several times, then dried in air at 60 °C for 10 h.

2.3. The Synthesis of β-$NaYF_4$:Yb,Er Nanocrystals (β-NYE NCs)

β-NYE products were prepared in a similar procedure, the difference is that the final reaction temperature is 320 °C and the heating rate was as fast as possible.

2.4. Characterizations

The crystal structures of the as-prepared products were analyzed by a Rigaku RU-200b X-ray powder diffraction (XRD) recorded at room temperature, the step scan covered the angular range from 10° to 70° with steps size of 0.02°, with a nickel-filtered Cu-Kα radiation ($\lambda =$ 1.5406 Å). The size and morphology were characterized by Transmission electron microscopy (TEM, JEOL 600) with an acceleration voltage of 200 kV. The upconversion emission (UC) spectra of the samples were recorded with a fluorescence spectrophotometer (Hitachi F-4500) under the excitation of a power-adjustable laser diode (980 nm, 0–2 W).

3. RESULTS AND DISCUSSION

3.1. Structural and Morphological Characterizations

The crystal structures of the as-prepared NYE NCs were characterized by the powder X-ray diffraction (XRD). As shown in Figure 1, the peak positions and intensities of the nanocrystals match well with those for the cubic α-NYE (JCPDS 06-0342) and the hexagonal β-NYE crystal (JCPDS 28-1192), respectively. No other peaks corresponding to other impurities were detected, which revealed that pure α-NYE and β-NYE had been fabricated. The peak broadening revealed the NCs nature for the as-prepared products.

The morphologies of the as-prepared NYE NCs were characterized by transmission electron microscopy (TEM). As we can see from the TEM images, the NYE NCs were well dispersed in cyclohexane because of the long-chain oleylamine ligands on the crystal surface. Figures 2(a) and (b) shows the typical TEM images of the α-NYE NCs and Figures 2(c) and (d) are the β-NYE NCs, both

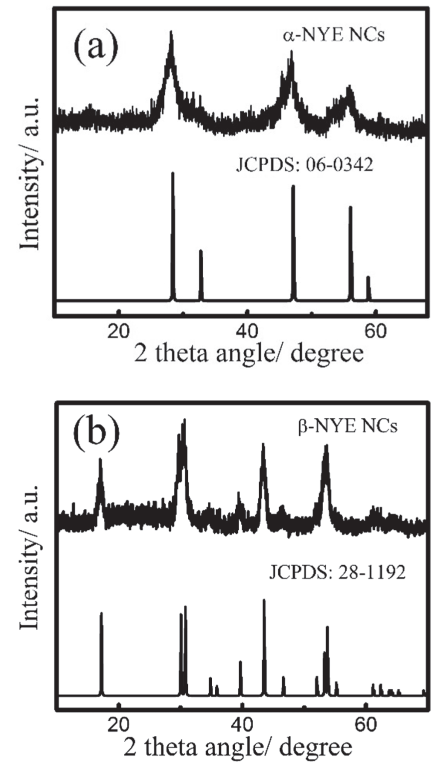

Figure 1. The XRD patterns of (a) α-NYE NCs and JCPDS 06-0342, (b) β-NYE NCs and JCPDS 28-1192.

of which with a uniform dimension of ~10 nm in diameter, obtained by random measurements of 200 particles from five TEM images. A dynamic light-scattering experiment showed that the average particle size is 10 ± 2 nm. Within the experimental uncertainty, the TEM and light-scattering results were consistent. In our experiment, the heating rate was as fast as possible, providing the reaction system enough energy to overcome the potential barrier between the cubic and hexagonal $NaYF_4$, while OA was

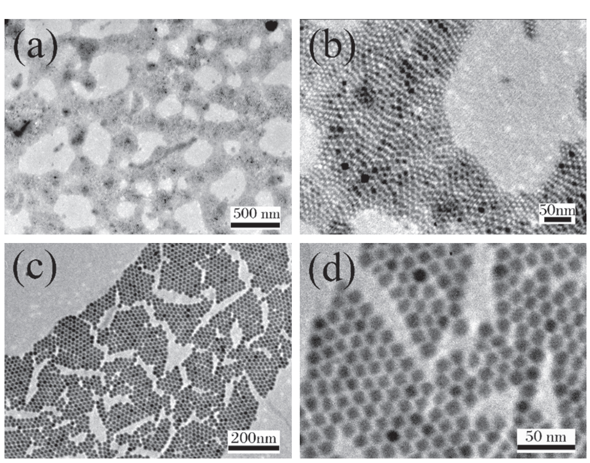

Figure 2. TEM image of the well-dispersed NYE nanocrystals with various magnifications: TEM image of α-NYE (a), and a higher magnification TEM image (b); TEM image of β-NYE (c), and a higher magnification TEM image (d).

used as a capping ligand to arrest the growth of the NCs and limit the particle size. So the α to β phase transformation occurred without a morphology evolution and a size change, that was the cubic particles converted to hexagonal particles.

3.2. Optical Properties

NYE is a typical upconversion luminescence material that can convert lower energy photons into higher energy photons through sequential absorption and energy transfer by the use existing intermediary energy states of lanthanide ions.[21, 22]

Figure 3 shows the photoluminescence emission spectra of the as-prepared α-NYE and β-NYE NCs under 980 nm NIR excitation (continuous wave (CW)). In the spectrum of the NYE nanocrystals, the four emission peaks located at 409 nm, 521 nm, 541 nm and 651 nm correspond to the $^2H_{9/2} \rightarrow {}^4I_{15/2}$, $^2H_{11/2} \rightarrow {}^4I_{15/2}$, $^4S_{3/2} \rightarrow {}^4I_{15/2}$, and $^4F_{9/2} \rightarrow {}^4I_{15/2}$ transitions of the Er^{3+} ions, respectively. The dominated green emission is centered at 541 nm for β-NYE NCs.

It was also found in Figure 3 that the phase transformation resulted in a large difference in the emission spectrum. The α to β phase transformation resulted in a significant enhancement in the intensities for the 541 nm emissions in the green region, while inducing a large reduction in the 651 nm in the red region.

3.3. Mechanism

Figure 4 describes the overall processes for the upconversion luminescence processes of Yb^{3+}–Er^{3+} co-doped NYE NCs under NIR excitation. We can recognize that the UC mechanism of the ~651 nm luminescence occurs via a two-step ET from Yb^{3+} to Er^{3+}. Firstly, under 980 nm excitation, the higher energy levels $^4I_{11/2}$ of the Er^{3+} ions are populated from the ground state $^4I_{15/2}$ via a successive energy transfer processes from neighboring Yb^{3+} ions to Er^{3+} and then populates the $^4I_{13/2}$ via non-radiative relaxation. Secondly, Er^{3+} ions in the $^4I_{13/2}$ state are excited to

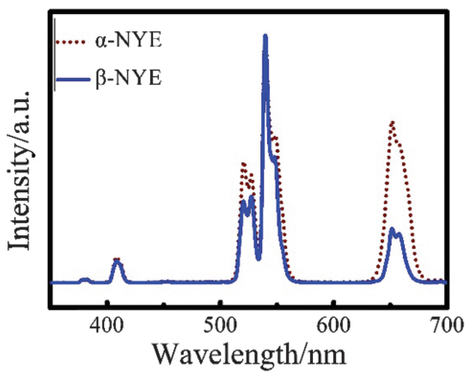

Figure 3. The upconversion photoluminescence (UCPL) spectra of the as-prepared α-NYE and β-NYE nanocrystals under 980 nm excitation at room temperature.

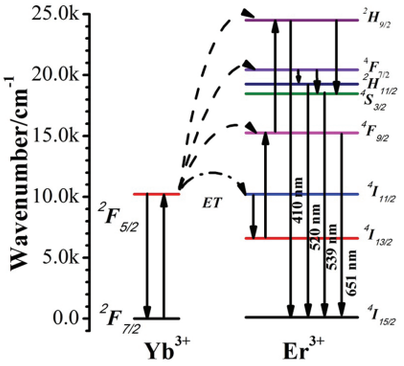

Figure 4. Diagrams of the energy levels of Yb^{3+}–Er^{3+} and the upconversion luminescence processes in an Yb^{3+}–Er^{3+} codoped system upon 980 nm excitation. The energy is transferred from Yb^{3+} to Er^{3+} through ET.

the $^4F_{9/2}$ states via another ET from excited Yb^{3+} ions, subsequently producing red (~651 nm) emissions. The $^4F_{7/2}$ and $^2H_{9/2}$ can also be populated from the $^4I_{11/2}$ and $^4F_{9/2}$ levels of the Er^{3+} ion by absorption a 980 nm photon, or energy transfer from an Yb^{3+} ion. Then the Er^{3+} ion can further non-radiatively relax and populate the $^2H_{11/2}$ and $^2S_{3/2}$ levels and afterwards produces the green (~520 nm, ~539 nm) emissions simultaneously. The radiative transitions from the populated $^2H_{9/2}$ level to the ground state $^4I_{15/2}$ can yield ~410 nm emissions through the cross relaxation processes between the Yb^{3+} and the Er^{3+} ion, although the $^2H_{9/2}$ level of Er^{3+} ions cannot be populated directly via an ET from excited Yb^{3+} to the Er^{3+} in the $^2H_{9/2}$ level due to a large energy mismatch.

4. CONCLUSION

In summary, uniform and well-dispersed upconverting lanthanide-doped α-$NaYF_4$:Yb^{3+},Er^{3+} and β-$NaYF_4$:Yb^{3+},Er^{3+} nanocrystals (NYE) with about 10 nm in diameter on average were prepared by thermal decomposition reaction using oleic acid as chelating agent and shape modifier. XRD, TEM and the UCPL spectra were used to characterize the material. In comparison, the α-NYE and the β-NYE NCs are capable of upconverting NIR light from a 980 nm diode laser into dominated red emissions (~651 nm) and green emissions (~521 nm), respectively, which probably are due to phase structure effect on the cross relaxation between Yb^{3+} and Er^{3+} ions. Their interesting characteristic thereby increases their commercialization possibilities to enable NYE based devices to meet more specific color demands. These upconverting nanocrystals have already been identified for potential applications in the field of optical display and solid-state laser.

Acknowledgment: This work was supported by the NSFC (grants Nos. 51072065, 61178073, and 61077033),

the Program for NCET in University (No: NCET-08-0243), the Opened Fund of the State Key Laboratory on Integrated Optoelectronics, and Tsinghua National Laboratory for Information Science and Technology (TNList) Cross-discipline Foundation.

References and Notes

1. L. L. Wang, X. J. Xue, F. Shi, D. Zhao, D. S. Zhang, K. Z. Zheng, G. F. Wang, C. F. He, R. Kim, and W. Qin, *Opt. Lett.* 34, 2781 (**2009**).
2. W. P. Qin, D. Zhao, J. S. Zhang, Y. Wang, C. Y. Cao, G. F. Wang, G. D. Wei, L. L. Wang, Y. Jin, L. F. Fu, P. F. Zhu, and S. Z. Lu, *J. Nanosci. Nanotechnol.* 8, 1464 (**2008**).
3. J. Mendez-Ramos, A. C. Yanes, A. Santana-Alonso, J. del-Castillo, and V. D. Rodriguez, *J. Nanosci. Nanotechnol.* 10, 1273 (**2010**).
4. W. Chen, *J. Nanosci. Nanotechnol.* 8, 1019 (**2008**).
5. Y. Liu, Q. Ju, and X. Chen, *Rev. Nanosci. Nanotechnol.* 1, 163 (**2012**).
6. L. Wang, Y. Li, Y. Zhang, H. Gu, and W. Chen, *Rev. Nanosci. Nanotechnol.* 3, 1 (**2014**).
7. X. J. Zhu, J. Zhou, M. Chen, M. Shi, W. Feng, and F. Y. Li, *Biomaterials* 33, 4618 (**2012**).
8. T. Yang, Y. Sun, Q. Liu, W. Feng, P. Yang, and F. Li, *Biomaterials* 33, 3733 (**2012**).
9. T. Y. Cao, T. S. Yang, Y. Gao, Y. Yang, H. Hu, and F. Y. Li, *Inorg. Chem. Commun.* 13, 392 (**2010**).
10. Q. Liu, W. Feng, T. S. Yang, T. Yi, and F. Y. Li, *Nat. Protoc.* 8, 2033 (**2013**).
11. X. Guo, W. Di, C. Chen, C. Liu, X. Wang, and W. Qin, *Dalton Transactions* 43, 1048 (**2014**).
12. X. Guo, W. Song, C. Chen, W. Di, and W. Qin, *PCCP* 15, 14681 (**2013**).
13. X. Guo, W. Song, J. Wang, F. Shi, and W. Qin, *J. Nanosci. Nanotechnol.* 14, 3726 (**2014**).
14. K. W. Kramer, D. Biner, G. Frei, H. U. Gudel, M. P. Hehlen, and S. R. Luthi, *Chem. Mater.* 16, 1244 (**2004**).
15. N. Menyuk, K. Dwight, and J. W. Pierce, *Appl. Phys. Lett.* 21, 159 (**1972**).
16. J. W. Zhao, Y. J. Sun, X. G. Kong, L. J. Tian, Y. Wang, L. P. Tu, J. L. Zhao, and H. Zhang, *J. Phys. Chem. B* 112, 15666 (**2008**).
17. E. Downing, L. Hesselink, J. Ralston, and R. Macfarlane, *Science* 273, 1185 (**1996**).
18. G. Yi, H. Lu, S. Zhao, Y. Ge, W. Yang, D. Chen, and L.-H. Guo, *Nano Lett.* 4, 2191 (**2004**).
19. F. Zhang, Y. Wan, Y. Shi, B. Tu, and D. Zhao, *Chem. Mater.* 20, 3778 (**2008**).
20. F. Shi, J. S. Wang, X. S. Zhai, D. Zhao, and W. P. Qin, *Crystengcomm.* 13, 3782 (**2011**).
21. D. M. Liu, D. Zhao, D. S. Zhang, K. Z. Zheng, and W. P. Qin, *J. Nanosci. Nanotechnol.* 11, 9770 (**2011**).
22. L. L. Wang, W. P. Qin, Y. Wang, G. F. Wang, C. Y. Cao, G. D. Wei, R. J. Kim, D. S. Zhang, F. H. Ding, and C. F. He, *J. Nanosci. Nanotechnol.* 10, 1825 (**2010**).

Received: 1 September 2014. Accepted: 4 June 2015.